Appl. Phys. B 62, 449–455 (1996)

Applied Physics B Lasers and Optics

A time-compensated spectral filter for transform-limited tunable picosecond pulse generation from spectro-temporal-selection dye lasers

N. D. Hung[1,3], Y. Segawa[1], Y. H. Meyer[2], P. Long[3], L. H. Hai[3]

[1] Photodynamic Research Center, The Institute of Physical and Chemical Research (RIKEN), 19-1399 Nagamachi Koeji, Aoba, Sendai 980, Japan
[2] Laboratoire de Photophysique Moleculaire (CNRS), Bat. 213, F-91405 Orsay, France
[3] Institute of Materials Sciences, National Centre for Sciences and Technology of Vietnam, Nghia do, Tu Liem, Hanoi, Vietnam
(Fax: + 84-4/352 483, E-mail: DAIHUNG@ims.ac.vn)

Received: 22 May 1995/Accepted: 11 December 1995

Abstract. Diffraction and transform-limited picosecond tunable pulses are generated from Spectro-temporal-Selection (STS) dye lasers by using a new extra-cavity filter. This filter is based on a grazing-incident grating and arranged in the configuration of a folded dispersive delay line. Thus, it provides both high spectral selectivity and controllable temporal compensation for elimination of pulse broadening. Direct production of diffraction- and transform-limited picosecond dye laser (10 μJ, 50 ps) pulses spectrally adjustable between 398 and 702 nm is demonstrated in a compact device, with 8 ns pump pulses from a nanosecond nitrogen laser.

PACS: 42.60.By; 42.55.MV

Ultrashort pulsed laser sources are of interest in a wide range of research applications [1–3]. Production of ultrashort laser pulses with micro-joule pulse energy is generally based on mode-locking techniques and requires the combined use of two expensive pump lasers, one CW, one pulsed. However, different methods to produce short pulses with a (non-mode-locked) nanosecond pump laser were proposed using the processes of cavity transients [4], cavity quenching [5], distributed feedback [6], and Spectro-Temporal Selection (STS) [7]. Considering the noticeable simplifications offered by these methods and the large number of nanosecond pump lasers currently available in spectroscopic laboratories, attention has been paid to their development [8–14]. The applicability of ultrashort laser pulses to some spectroscopic or nonlinear optical experiments depends not only on pulse duration but also on different characteristics: wavelength tunability, spatial and spectroscopic quality as well as stability in pulse duration and energy. We show here the improvements on such characteristics of picosecond STS dye lasers.

The principle of the STS method is based on a fast spectral evolution in the broad-band laser emission of a short and low-Q dye laser oscillator, and technically it is to select with an extra-cavity filter a narrow spectral band on the short-wavelength side of this broadband laser spectrum in order to produce single picosecond pulses [7, 11–14]. In the early reports, a Littrow grating was used as an extra-cavity spectral filter which presented three disadvantages: (1) considerable pulse broadenings introduced by the grating and the delay across dye-laser beam width: (2) low spectral selectivity of the filter that made the spectral bandwidths of the STS picosecond laser ($\sim 10\,\mathrm{cm}^{-1}$ FWHM) much greater (50 times) than the Fourier-transform limit set by pulse durations; (3) requirement of optical realignments during the wavelength tunability because the grating rotation led to the variation of output laser beam direction.

The pulse broadening resulting from the angular dispersion of a grating was studied by some authors [15–18]. The pulse broadening due to the delay across the laser beam width when a reflection grating is used as a single-pass spectral filter can be evaluated from simple geometrical calculations by the following formula:

$$\Delta t = \frac{k\lambda D}{ca\cos i},$$

where Δt is the delay across laser beam width: λ is the laser wavelength; D is the laser beam width; k is the diffraction order; a is the grating constant; c is the light speed in vacuum and i is the incident angle. In the case of a Littrow grating, (1) is simply expressed by

$$\Delta t_{\mathrm{Littrow}} = \frac{2D\tan i}{c}.$$

Thus an STS dye laser that uses a 2400 groove/mm grating and ~ 1.5 mm laser beam diameter, suffers from the pulse broadening (due to the delay across the laser beam width) which range from 7 to 18 ps depending on the laser wavelength in the visible spectrum.

Spectral linewidth of STS picosecond laser pulses depends only on the extra-cavity filter. The single-pass selectivity of extra-cavity filter can be enhanced by either combining the selective properties of addition filters or using beam expanders. However, such spectral filter systems cause not only pulse broadening but disadvantages

in wavelength tuning, optical arrangement and extra cost. Remarkably, the beam expansion with a single grazing incidence grating can provide large beam expansion [19, 20], the beam expansion factor (M) is approximately given by

$$M \approx \cos i/\cos \beta$$

here, i is the Littrow angle of the grating and β the grazing incident angle ($\sim 90°$). As a result, a single grazing incidence grating configuration could achieve a single-pass linewidth which is almost a factor of 100 narrower than that of the Littrow configuration, grazing-incidence grating dye lasers generated pulses of linewidth of 0.1 cm^{-1} (FWHM) or even narrower with the modified grazing-incident configurations [19–22]. However, such grazing grating configurations cannot be directly applied to the STS picosecond dye lasers because a dramatic pulse broadening due to delay across the laser beam width is M times greater than that of a Littrow grating [see (1) and (3)].

In this paper, we report for the first time the use of a grazing incident grating as an extra-cavity spectral filter for picosecond STS dye lasers. The filter is arranged in the folded dispersive delay line configuration in order to provide both a very high spectral selectivity and controllable temporal compensation for an elimination of pulse broadening. These allow one to overcome the above-mentioned disadvantages in order to produce nearly diffraction and transform-limited picosecond tunable pulses from STS dye lasers.

1 Experimental

1.1 Description and analysis of filter

The basic requirement to design a temporally compensated spectral filter is to use a double-function configuration that allows one to obtain both a high spectral selectivity and controllable temporal compensation for an elimination of pulse broadening.

The grating-based filter configuration shown in Fig. 1, consists of a holographic grating (G) operated at a grazing incident angle of $\sim 89°$, an antireflection-coated lens (L4) and an aluminum stripe mirror (TM) of ~ 0.15 mm width. The lens L4 and stripe mirror TM were placed on a moveable platform to vary the spacing between them and the grating G. The stripe mirror TM can be moved horizontally, in the focal plane of the lens L4, with respect to the grating groove. The beam to be filtered (coming beam) passes through the grating G, lens L4 and stripe mirror, the filtered beam (returning beam) is reflected back with the stripe mirror and passes through the setup a second time.

The grating (grazing incidence for the first diffraction order only) was selected to be such that: $\lambda/2 < a/2 < \lambda$, here a is the grating constant, which ensures both a high spectral selectivity and an elimination of the losses due to different unwanted diffraction orders. Considering the diffraction gratings available in our laboratory and the wavelength tuning over the visible spectral range, we used a Jobin-Yvon, 2400 g/mm grating. The diffracted light was

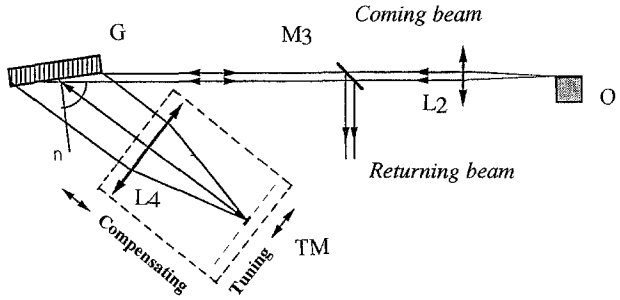

Fig. 1. Top view of extra-cavity filter with a grazing incidence grating arranged in folded dispersion delay line configuration (*O*: untuned low-Q dye-laser oscillator; *L2*: collimating lens; *G*: holographic grating (2400 g/mm); *L4*: antireflection-coated lens: *TM*: stripe tuning mirror); *M3*: returning mirror. To avoid the losses due to the use of a beam splitter, the returning beam was shifted from the coming beam direction, with a slight tilt of the stripe mirror in vertical direction and then driven by mirror M3

focused by the lens L4 ($f = 15$ cm) on the stripe mirror, as shown in Fig. 1. The selected wavelength is determined by the stripe mirror position and wavelength tunability is obtained by translating the stripe mirror horizontally, in the focal plane of the lens L4, with respect to the grating groove. No optical realignment is required during the wavelength tuning. In such a filtering configuration, the beam expansion factor achievable is 50 times; a single-pass spectral selectivity of 0.2 cm^{-1} (FWHM) is expected.

The combination of the grating, lens L4 and the stripe mirror forms a folded grating pair compressor with an internal telescope of angular magnification equal to 1. This configuration was studied in detail by Martinez et al. [23, 24]. The linear dispersion in this delay line (compressor) can be continuously tuned by varying the spacing between the grating G and the ensemble lens L4 and stripe mirror, the effective dispersion length was expressed by (8) of Ref. [24]:

$$l_{\text{eff}} = [l - 2(f_1 + f_2)]A^2,$$

where the angular magnification A of the telescope is defined by: $A = f_1/f_2; f_1, f_2$ are the focal lengths of the two lenses. l_{eff} and l are the effective length of dispersion and the distance between two gratings, respectively (in our case, l is 2 times larger than the spacing between the grating G and the stripe mirror). This equation also shows that l_{eff} can be negative. Thus, by varying the spacing between the grating G and the ensemble lens L4 and the stripe mirror we may have negative, zero and positive values for the group velocity dispersion. As a result, the returning beam reflected back by the stripe mirror can be temporally compensated to eliminate the pulse broadening introduced by the grating during the spectral selection.

1.2 Transform-limited picosecond STS dye laser

The present STS dye laser shown in Fig. 2 is compact: 30×35 cm. The STS oscillator (O) is simply a standard 1×1 cm spectroscopy cell which constitutes a low-Q cavity of 120 ps round-trip time between the uncoated external faces (0.04 reflectivity). The oscillator is

transversally excited through a cylindrical lens of 5 cm focal length, by a small part (~1 mJ) of the output (8 ns, 9 mJ at 337 nm, 15 Hz) from a TE nitrogen laser (NL-1000). The output from the STS oscillator is collimated by a 10 cm lens (L1) and directed into the extra-cavity grating-based filter. Avoiding losses due to the use of beam splitters, the returning beam was shifted from the coming beam direction with a slight tilt (<35 mrad) of the stripe mirror in vertical direction and then driven into the multipass amplifier (MPA) by the mirror M3. The influence of this tilt (compressor misalignment) on temporal compressibility is evaluated as in [25] to be about 260 fs (uncompressed time due to residual dispersion) which cannot be neglected for subpicosecond pulse duration, but can for this STS picosecond dye-laser pulse. The multipass amplifier (MPA) was pumped by the same nitrogen laser. The wavelength tuning is obtained with the horizontal translation of the stripe mirror in the focal plane of lens L4. No optical realignment is required during the wavelength tuning. A Polaroid half-wave plate (HW) is used in order to optimize the diffracted intensities from the grating and the amplification in the MPA. All mirrors have 10 mm diameters and aluminum coatings.

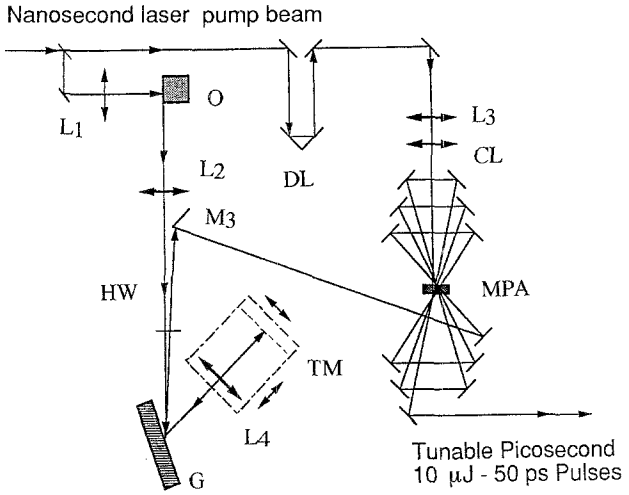

Fig. 2. The STS dye laser for generation of transform-limited picosecond tunable pulses with a nanosecond pump. *O*: low-Q dye-laser oscillator; *CL*: cylindrical lens; *L*: lens, *G*: grating; *HW*: halfwave plate; *DL*: optical delay line; *MPA*: 6-pass amplifier

The amplifier MPA is a 1 mm path cell, standard circulation Hellma model, longitudinally pumped with >4 mJ focused in a ~1 mm diameter spot through a spherical (10 cm f.l.) and a cylindrical (8 cm f.l.) lens. The latter lens was needed to reshape the excitation spot on the MPA cell with respect to the initial rectangular section of the nitrogen laser beam. The distance between the first and sixth pass is 76 cm. The path from the oscillator O to the MPA is adjusted with the optical delay line (DL) for amplifying all six passes by the maximum of the pump pulse at the multipass amplifier cell. The value of the saturated total gain of the six-pass amplifier (MPA) is found to be about 3.6×10^3 with Rhodamine dyes. The shot to shot stability in intensity of the picosecond STS pulses is found to be much better after amplification if saturated amplification is established in the 6-pass amplifier (see 2.3 Sect). The STS picosecond pulse energy is typically 10 μJ (15 μJ for rhodamine dye solutions). It is straightforward to further amplify the 10 μJ picosecond output STS laser pulses with additional dye amplifiers to obtain high-energy picosecond pulses.

The time effect of spectral selection in the STS lasers is as follows: when the stripe mirror TM is translated for tuning at the maximum of the laser broad-band spectrum, the output pulse is several nanoseconds long. When the stripe mirror TM is tuned to the blue wing of the oscillator broad-band, the output pulse becomes shorter and at a given wavelength a single (<80 ps) picosecond peak is produced. The shortest pulse width is obtained with a slight variation of the spacing between the grating and the ensemble lens L4 and the stripe mirror.

We have tested the production of picosecond pulses with this STS laser with 17 different dyes from Exciton (listed in Table 1) which differently absorb the pumping

Table 1. Characteristics of picosecond STS dye lasers with the temporally compensated spectral filter

Dye (solvent)	Tuning range (nm)	Concent. (10^{-3} M/l)	Pulse duration (ps)	Output energy (μJ)	$\Delta\sqrt{}$ (cm^{-1})
Nile blue 690 (EtOH)	696–702	0.6–7	54	5	0.27
Cresyl violet (EtOH)	663–668	6–25	56	5	0.26
DCM (DMSO)	652–657	3–37	55	9	0.25
Rhodamine 640 (EtOH)	624–653	1–16	45	13	0.24
Rhodamine 610 (EtOH)	594–623	1–14	47	15	0.24
Rhodamine 590 (EtOH)	561–586	0.2–7	45	16	0.24
Rhodamine 110 (EtOH) (Lambda Physik)	545–557	0.8–15	48	15	0.24
Disodium fluorescein	528–542	0.4–5	50	13	0.24
Coumarin 540A (EtOH)	521–529	3–16	53	12	0.24
Coumarin 503 (EtOH)	496–504	4–16	55	10	0.24
Coumarin 481 (*p*-Dioxane)	478–484	4–13	54	9	0.24
Coumarin 480 (EtOH)	465–473	1–25	55	8	0.24
Coumarin 460 (EtOH)	453–456	0.5–2.1	50	8	0.24
Coumarin 440 (EtOH)	431–439	0.5–1.6	54	7	0.24
Stilbene 420 (MeOH)	419–426	0.1–0.5	55	7	0.24
POPOP (*p*-Dioxane)	412–418	0.3–0.9	52	7	0.24
DPS (*p*-Dioxane)	398–403	0.1–0.8	54	5	0.25

wavelength 337 nm. The output pulse shape of the STS laser is monitored by a Hamamatsu streak camera of 3 ps resolution. The average picosecond pulse durations produced at the 15 Hz repetition rate are measured by the autocorrelation method of non-collinear second harmonic generation. The pulse energies are measured with pyroelectric energy detectors of Laser energy meters (Scientech - 362 and Ophir) and spectral parameters with a monochromator SPEX-1402 and Fabry-Perot etalons.

2 Results and discussion

We have successfully operated this STS laser with the 17 different dyes pumped at 337 nm to generate diffraction and transform-limited picosecond pulses (~ 50 ps) adjustable in the wavelength range from 398 to 702 nm. The STS laser operating characteristics are given in Table 1.

2.1 Transform-limited picosecond STS pulse

The present grating-based filter configuration is entirely equal to that of a folded grating compressor with an internal telescope and a stripe mirror. Its linear dispersion can be tuned by varying the spacing between the grating and the ensemble lens L4 and stripe mirror TM. The zero dispersion point is the point where the distance of lens L4 to the grating is equal to that of this lens to the stripe mirror [23]. Thus this point is chosen as an initial working point of the filter. When the stripe mirror was translated from the maximum of the laser broad-band spectrum to its blue wing, the filtered STS pulse duration shortened from several nanosecond down to sub-100 ps. The shortest STS pulse duration was obtained with a slight variation (within 3 mm) of the initial working point. This possibly results from either a coarse position of the zero dispersion point (initial working point) or a lack of parallelism in the coming beam. Figure 3 shows the autocorrelation traces of the imperfectly and perfectly compensated pulses at 603 nm and the compensated pulse at 540 nm. The pulse widths are found for a sech^2-shaped pulse to be 62, 45 and 50 ps, respectively. These values are in a good agreement with the averaged pulse duration statistically measured by the streak camera (Fig. 5). This partially results from the improved stability of pulse duration when the smooth pumping pulse is used for the STS method. As presented below, the stability in the output pulse duration measured to be $\pm$ 7% rms which is nearly 2 times better than that of the multimode Nd : YAG laser pumping [12].

The compensated STS pulse durations obtained at different laser picosecond wavelengths between 398 and 702 nm are presented in Table 1. They are the shortest tunable pulses obtained from STS picosecond dye lasers and in good agreement with the pulse duration values calculated with a smooth pulse pumping [13, 14].

2.2 Tunability, spectral and spatial quality of picosecond STS pulse

For the shortest pulse width at a given laser operation, we could continuously tune wavelength over ~ 3 nm range with negligible pulse width variations. A broad spectrally adjustable STS picosecond dye laser was obtained by translating the stripe mirror to the desired wavelength and then by varying the dye concentration to achieve the shortest pulse.

We found, with all rhodamine dyes used, that the highest dye concentration was one order of magnitude larger of 337 nm ($\varepsilon \sim 0.3 \times 10^4$ l M^{-1} cm^{-1}) than for 532 nm ($\varepsilon \sim 5 \times 10^4$ l M^{-1} cm^{-1}) pumping [12]. Correspondingly, the widest tunability range, namely 29 nm, was obtained with Rhodamine dyes. This has resulted from the fact that the tuning range of the picosecond STS pulse wavelength, at a given pumping energy, is limited by the dye concentration range in which (broad band) laser action occurs in the short and low-Q dye oscillator. Thus, the use of the ultraviolet excitation for the STS lasers containing rhodamine dye solutions which moderately absorb at 337 nm, widened the usable dye concentration range and, therefore, the tuning range of picosecond pulse wavelength.

The output of the picosecond STS dye laser was analyzed by a 6 mm solid Fabry-Perot etalon having a FSR of

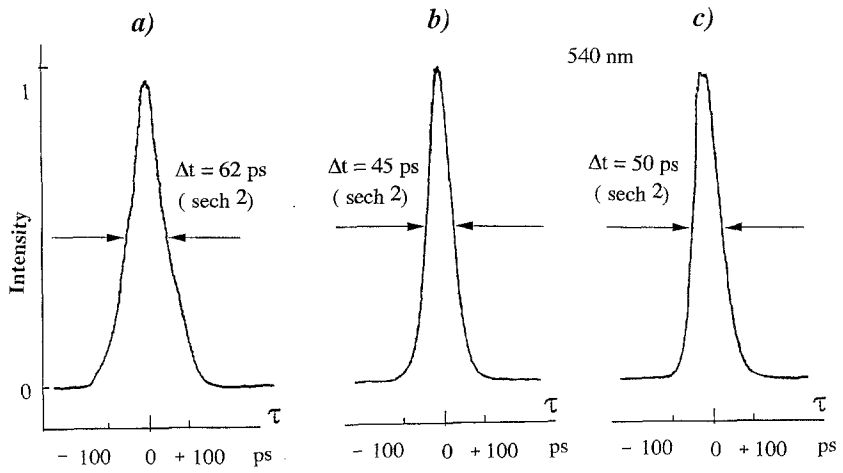

Fig. 3a–c. Autocorrelation traces of the output STS laser pulses (**a**) imperfectly, (**b**) perfectly compensated for the Rhodamine 610 laser at 603 nm; (**c**) for the Disodium Fluorescein laser at 540 nm. The pulse widths were found for a sech^2-shaped pulse fits to be 62, 45 and 50 ps, respectively

17 GHz and a finesse of 26 in the visible spectral range. The rings, shown in Fig. 4a and b, were obtained through this etalon with 60 s exposure at a repetition rate of 15 Hz. These show time-averaged linewidths of 0.24 cm^{-1} for the laser picosecond wavelengths at 540 and 603 nm. The spectral linewidth increases little as the wavelength of operation increases. The spectral linewidth values, as shown in Table 1, were measured to be nearly conserved during the wavelength tuning of the picosecond STS laser output. The time-bandwidth products are smaller than 0.37 which is 1.2 times that of the transform-limited value for a $sech^2$-shaped pulse.

When transform-limited operation is not required, spectral linewidth can be changed by varying either stripe mirror width or incident angle. The stripe mirror width is possibly varied by the use of a wedge-shaped slit that is placed in contact with a stripe mirror. Separate measurements at 632.8 nm (He–Ne), 488 and 514.5 nm (Ar ion laser) showed that the feedback reflection of the grating-based filter ($\beta = 89°$) is about 26% for the laser light polarized horizontally to the grating groove. The losses through the filter are mainly caused by the grating reflections. When incidence angle is decreased to values smaller than 75°, the efficient feedback reflection achievable is nearly 80%. Such a value makes the filter configuration attractive to many other applications.

Resulting from both a diaphragm effect in the multipass amplifier and the use of a stripe mirror in the extra-cavity grating filter, the quality of the output amplified beam was measured to be excellent. The beam divergence reduce from 2.5 mrad [11–14] down to 1.0 mrad, the value is the diffraction limit considering the STS dye beam waist ($\sim$0.1 mm).

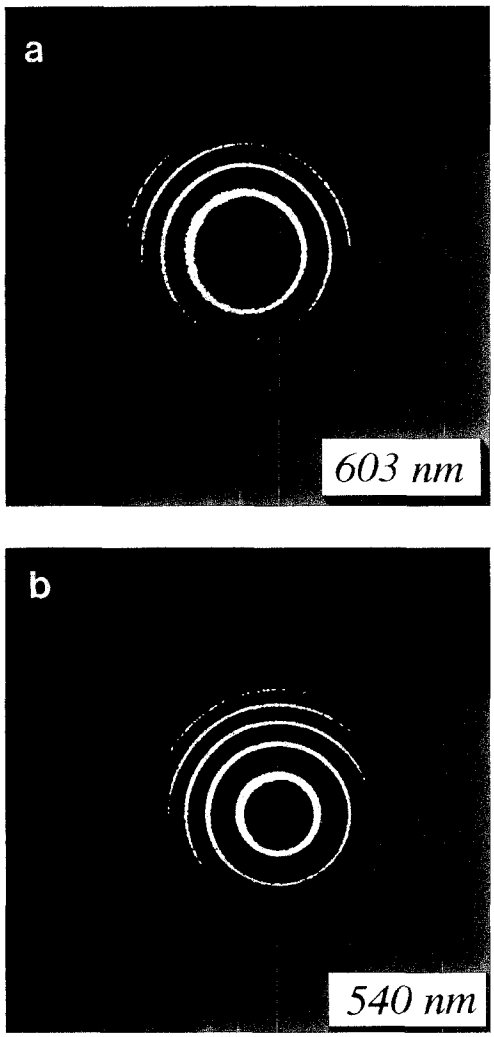

Fig. 4a, b. Fabry-Perot patterns of picosecond STS laser radiations (60 s exposure) (**a**) at 603 nm and (**b**) at 540 nm. Free spectral range of the Fabry-Perot etalon is 17 GHz. The time averaged linewidth is 0.24 cm^{-1} (FWHM) for the radiations

2.3 Picosecond pulse intensity and duration fluctuations

The main reason for the fluctuation in pulse intensity and duration of picosecond STS lasers is the fact that they were pumped by highly structured pulses (due to mode beating) from multimode Nd:YAG lasers, these fluctuation measures were $\pm$ 15% rms [12]. This led us to consider the output stability of the picosecond STS lasers pumped by the smooth pulses emitted from the nitrogen laser.

As mentioned above, the operational conditions of the multipass amplifiers (MPA) can improve the shot to shot intensity stability of the picosecond STS pulses avoiding a reduction in the total gain available. We adjusted pump energy, dye concentration and signal amplitude so that saturated amplification is established in the final passes. When the pumping pulse of $\sim$5 mJ energy was focused on a $\sim$1 mm diameter spot in the MPA, the pumping intensity averaged over 8 ns is 45 MW/cm^2, which is $\sim$3 times greater than the steady-state saturation intensity (I_s) of the Rhodamine dye solution at 337 nm: $I_s = h\nu/\sigma_a\tau_{fluo} = 2.3$ MW/cm^2 with $\tau_{fluo} = 4$ ns and $\sigma_a \sim 0.5 \times 10^{-17}$ cm^2.

We have studied the stability degree of the output pulse duration and energy in the case of Rhodamine 610 dye. Within the pumping range of 3 to 10 times above the lasing threshold of the oscillator O, the average duration of the output pulse was measured by autocorrelation not to be influenced by the pump laser power. Pumping energy more than 10 times above threshold is impossible because of the insufficient nitrogen laser energy available. This is unlike other picosecond laser pulse production methods which generally operate close to threshold [4–6].

The output of this laser was recorded by a streak camera of 3 ps resolution. Eight-hundred pulse traces were sampled and each FWHM duration and intensity were recorded. Figure 5 indicates the statistics for the Rh 610 laser output pulse duration. The average pulse duration is found to be 45 ps, the stability in pulse duration is $\pm$ 7% rms. The average pulse duration obtained with the streak camera in the statistic measurement is in a fair agreement with that of the autocorrelation measurement. The effect of pulse to pulse variation on the measured autocorrelation function that had averaged a large number of individual pulses [26], is possibly insensitive in such pulse duration stability ($\pm$7% rms). We measured the stability in the output pulse intensity to be $\pm$9% rms, this

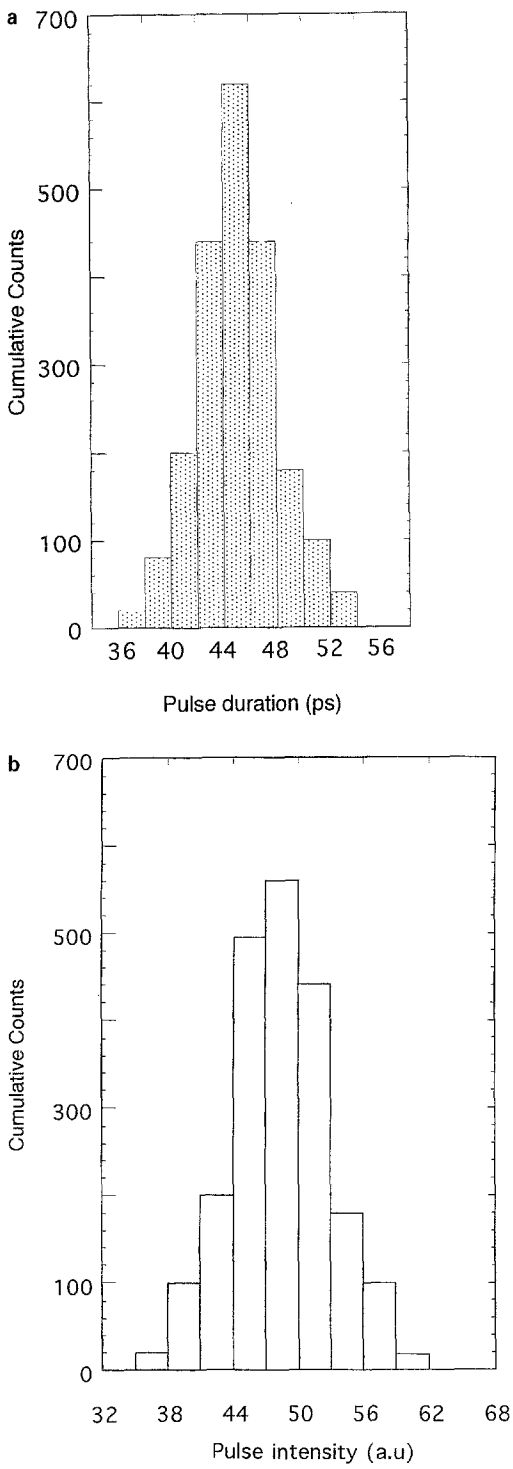

Fig. 5a, b. Statistics of the output pulse duration (**a**) and the output pulse intensity (**b**) of the rhodamine 610 STS dye laser. Stabilities are found to be $\pm 7\%$ rms and $\pm 9\%$ rms, respectively

value is strongly dependent on the operational condition of the MPA. Both the values of output stability are comparable to those of the tests with pumping by the smooth pulse emitted from a single-mode injected Nd : YAG laser (Quantel) [12]. The result shows that the use of smooth pumping pulse offers a large increase of stability (both in pulse duration and energy) with a factor of 2 times over that of the multimode Nd : YAG laser pumping [12].

3 Conclusion

Apart from demonstrating of the advantage of the use of smooth pumping pulse for the output stability of picosecond STS laser, we have presented a new extra-cavity high-selectivity filter for tunable picosecond STS dye lasers. The filter was based on a grazing incidence grating and arranged in the folded dispersion delay-line configuration with a stripe mirror. The experimental results show the important advantages of this spectral filter. First, it provides spectral and spatial high selectivity with a single grating. Second, it is a device of continuously tunable dispersion to provide temporal compensation during wavelength tuning of spectrally filtered short optical pulses. Third, it is very convenient for broad and continuous wavelength tuning with simple translation of the stripe mirror. These advantages do not only lead to the generation of nearly diffracting and transform-limited picosecond tunable pulses from STS dye lasers, but also make the filter attractive for other applications to ultrashort laser pulse techniques such as spectral filtering of ultrafast supercontinuum, dispersion compensation of short pulse laser cavities.

From these results we designed a compact picosecond device (30×35 cm) for converting fixed-wavelength nanosecond pulses emitted from a standard nanosecond laser (such as Nd : YAG, ruby, nitrogen, excimer lasers) into diffraction and transform-limited picosecond pulses spectrally adjustable in the visible spectral range.

Acknowledgement. N. D. Hung wishes to acknowledge the support received from the STA Program of the Research Development Corporation of Japan (JRDC).

References

1. W. Kaiser: *Ultrashort Laser Pulses. Generation and Applications*, 2nd edn., Topics Appl. Phys., Vol. 60 (Springer, Berlin, Heidelberg 1993)
2. F.P. Schäfer (ed.): *Dye Lasers*, 3rd edn., Topics Appl. Phys., Vol. 1 (Springer, Berlin, Heidelberg 1990)
3. F.J. Duarte, L.W. Hillman (eds.): *Dye Laser Principles* (Academic, New York 1990) F.J. Duarte, J.A. Paisner, A. Penzkofer: Appl. Opt. **31**, 33 (1992)
4. C. Lin, C.V. Shank: Appl. Phys. Lett. **26**, 389 (1975)
5. F.P. Schäfer, L. Wenchong, S. Szatmari: Appl. Phys. B **32**, 123 (1983)
6. Z. S. Bor, A. Müller, B. Racz, F.P. Schäfer: Appl. Phys. B **27**, 9 (1982); Appl. Phys. B **27**, 77 (1982)
7. M.M. Martin, E . Breheret, Y.H. Meyer: Opt. Commun. **56**, 61 (1985)
8. N. Sarakura, Z. Liu, Y. Segawa, M.A. Dubinskii, Opt. Lett. **20**, 599 (1995)
9. S. Yoshikawa, T. Imasaka: Jpn. J. Appl. Phys. **33**, 4898 (1994)
10. D.L. Hatten, Y. Cui, W.T. Hill, T. Mikes, J. Goldhar: Appl. Opt. **33**, 7042 (1992)
11. N.D. Hung, Y.H. Meyer, M.M. Martin, F. Nesa: In *Ultrafast Phenomena in Spectroscopy*, ed. by E. Klose, B. Wilhelmi, Springer Proc. Phys., Vol. 49 (Springer, Berlin, Heidelberg 1990) p. 33
12. N.D. Hung, Y.H. Meyer: Appl. Phys. B **53**, 226 (1991)
13. N.D. Hung, P. Plaza, M. Martin, Y.H. Meyer: Appl. Opt. **33**, 7046 (1992)

14. N.D. Hung, Y. Meyer, P. Long: SPIE Proc. **2321**, 286 (1994)
15. E.B. Treacy: IEEE J. QE-**5**, 454 (1969)
16. Zs. Bor, B. Racz: Opt. Commun. **54**, 165 (1985)
17. O.E. Martinez: Opt. Commun. **59**, 229 (1984)
18. O.E. Martinez: J. Opt. Soc. Am. B **3**, 929 (1986)
19. M. Littman, H. Metcalf: Appl. Opt. **17**, 2224 (1978)
20. I. Shoshan, N.N. Danon, U.P. Oppenheim: J. Appl. Phys. **48**, 4495 (1977).
21. N.D. Hung, P. Brechignac: Appl. Opt. **27**, 1906 (1988)
22. N.D. Hung, P. Brechignac: Opt. Commun. **54**, 151 (1985); N.D. Hung, P. Brechignac, C. Bruno: Appl. Phys. B **51**, 75 (1990)
23. O.E. Martinez: IEEE J. QE-**23**, 59 (1985)
24. O.E. Martinez, J.P. Gordon, R.L. Fork: J. Opt. Soc. Am. A **10**, 1003 (1984)
25. K. Osvay, I.N. Ross: Opt. Commun. **105**, 271 (1994)
26. E.W. Van Stryland: Opt. Commun. **31**, 93 (1979)